Supporting Information for

Dual strategies of mild C-F scissoring fluorination and local high-concentration electrolyte to enable reversible Li-Fe-F conversion batteries

Yifan Yu [1,2,3,§], Chuanzhong Lai [1,2,3,§], Meng Lei [1,2,3], Keyi Chen [1,3], Chilin Li [1,2,3,*]

[1] State Key Laboratory of High Performance Ceramics and Superfine Microstructure, Shanghai Institute of Ceramics, Chinese Academy of Sciences, 585 He Shuo Road, Shanghai 201899, China. Email: chilinli@mail.sic.ac.cn

[2] Center of Materials Science and Optoelectronics Engineering, University of Chinese Academy of Sciences, Beijing 100049, China.

[3] CAS Key Laboratory of Materials for Energy Conversion, Shanghai Institute of Ceramics, Chinese Academy of Sciences, Shanghai 201899, China.

[§] Y. Yu and C. Lai contribute equally to this work.

Experiments

Synthesis of iron-based fluorides. Iron-based fluorides were synthesized based on the hydrodefluorination of CF_x (XFNANO, >99.5%). Specifically, 200 mg CF_x and 2 mmol $FeCl_3 \cdot 6H_2O$ (Aladdin, 98%) were added into the polytetrafluoroethylene (PTFE) bottle, followed by the addition of 8 mL benzylamine (Alfa, ≥ 98.5%). Subsequently, the mixture was stirred at 95 ℃ for different reaction time (i.e., 12, 24 and 36 h). The black products were washed by acetone and alcohol and then centrifuged with a speed of 5000 rpm for 3 min, and these processes were repeated several times. The products were then dried in a vacuum oven at 80 ℃ overnight, and then they were transferred into furnace and heated at 300 ℃ for 2 h in a N_2 atmosphere. The final products (i.e. the mixture of HTB-FeF_3 and tetragonal FeF_2) after heat treatment were named as FF-12, FF-24 and FF-36, corresponding to the fluoride composites obtained based on different reaction times of 12, 24 and 36 h, respectively. In order to confirm the capacity contribution of

the defluorinated product of CF_x, the FF-24 was soaked in the dilute hydrofluoric acid solution to remove the iron-based fluoride. The residual solid was washed, dried and heated based on the same procedure as FF-24.

Preparation of electrolytes. A general electrolyte was prepared by dissolving 287.1 mg lithium bis(trifluoromethanesulphonyl)imide (LiTFSI, Sigma-Aldrich) into 500 μL 1,3-dioxolane (DOL, Aladdin, 99.8%) and 500 μL dimethyl ether (DME, Sigma-Aldrich, 99.5%), and it is abbreviated as LDD. The modified electrolyte was prepared by dissolving 287.1 mg LiTFSI into the mixed solvent of 200 μL diethylene glycol dimethyl ether (G2, Aladdin, 99.5%) and 800 μL 1H,1H,5H-Perfluoropentyl-1,1,2,2-tetrafluoroethylether (OFE, Aladdin, 98%), and it is abbreviated as LGO. Another modified electrolyte was prepared by dissolving 0.0287 g lithium difluoro(oxalato)borate (LiDFOB) into LGO, and it is abbreviated as LLGO.

Preparation of cathodes and assembly of cells. Poly(vinyl difluoride) (PVDF, Sigma-Aldrich) was employed as the binder and dissolved in N-Methyl pyrrolidone (NMP, Sinopharm Chemical Reagent Co., Ltd, ≧99.0%) to obtain the solution of 1 mg PVDF in 20 μL NMP. The cathodes were prepared by mixing the active material (FF-12, FF-24, or FF-36), conductive carbon (Super P, MTI Corporation) and PVDF with a mass ratio of 8:1:1. Then the mixture was pasted on Al foil and dried in vacuum at 80 ℃ overnight. For the evaluation of electrochemical performance of iron-based fluorides, the fluoride cathode, celgard2400 separator (Φ = 19 mm), lithium foil anode (Φ = 12 mm), stainless steel (SS) current collectors, and spring sheets were placed in the cell case in sequence with the injection of 30 μL electrolyte. For the measurements of liner sweep voltammetry (LSV) and step-wise potential sweeping (SWPS), the configuration of SS||electrolyte||Li cell was used. As for the Li||LDD/LLGO||Cu cells, the Cu foil electrode was cut into a disk shape with Φ = 19 mm and then washed by dilute hydrochloric acid, followed by drying in a vacuum at 80 ℃. All these cells were fabricated in an Ar filled glove box (O_2, H_2O < 0.1 ppm, Vigor).

Characterizations of morphology and structure. The structure and phase composition of powder were confirmed by X-ray diffractometer (XRD, Bruker, D8 Discover) in a scanning 2θ range of 10-80 °. The evolutions of morphology and crystal structure of electrodes were monitored by scanning electron microscopy (SEM, Magellan 400L, FEI) and transmission electron microscopy (TEM, JEOL JSM-6700F) with an acceleration voltage of 200 kV. The X-ray photoelectron spectroscopy (XPS, ESCAlab-250) with an Al anode source was employed to analyze the valence and surface composition of FF-24 at the pristine, 5^{th}-discharged and 5^{th}-charged states. The Raman spectra with an excitation light source wavelength of 532 nm were used to analyze the solvation structures of different electrolytes as well as the defluorination products of CF_x with and without the presence of $FeCl_3$.

Measurements of electrochemical performance. The galvanostatic charge and discharge curves in a voltage range of 1.2-4.0 V vs. Li/Li^+ were obtained on the Land multichannel battery testing system (CT2001A) at room temperature (RT). The galvanostatic intermittent titration technique (GITT) was carried out at a low current density of 30 mA g^{-1} with the following relaxation process for 6 h to reach a relatively equilibrium state. For the cyclic voltammetry (CV) test in 1.2-4.0 V vs. Li/Li^+, the scan rate was changed from 0.2 to 1.0 mV s^{-1}. The CV tests were performed on an electrochemical workstation (Princeton Versa STAT3). The electrochemical stability of electrolytes was analyzed by LSV and SWPS. The LSV test was carried out at a scan rate of 1 mV s^{-1}. The SWPS test was conducted on the SS||Li asymmetric cells, which were charged to and kept at a constant voltage of 4.1, 4.2, 4.3, 4.4, 4.5, 4.6, 4.7, 4.8, 4.9 and 5.0 V for 1 h, respectively. The transference number of Li^+ (t_+) of electrolytes was measured by using a Li||Li symmetric cell with a direct current (DC) polarization voltage of 0.01 V on the electrochemical workstation. And the t_+ value was calculated by the following equation:

$$t_+ = \frac{I_{ss}(\Delta V - I_0 R_0)}{I_0(\Delta V - I_{ss} R_{ss})}$$

where ΔV is the polarization voltage (i.e., 0.01 V), I_0 and R_0 represent the initial current

and resistance before polarization, respectively. I_{ss} and R_{ss} denote the stable current and resistance after polarization, respectively. The stability of Li metal anode was evaluated by the average coulombic efficiency measurement of Li||Cu cells. Specifically, the Li||Cu cells with different electrolytes were firstly discharged for 10 h at 0.2 mA cm^{-2} and then charged to 1.0 V to realize the complete stripping of Li from the Cu foil. Subsequently, the cells continued to discharge for 10 h at 0.2 mA cm^{-2} and then a ten plating/stripping cycles with an area capacity of 0.5 mA h cm^{-2} at 0.5mA cm^{-2} were conducted on these cells. Finally, the cells were charged to 1.0 V.

Theoretical calculations. The HOMO-LUMO calculation of solvent molecules and Li salts were conducted by Gaussion 09 package. The optimizations of structure and energy were carried out by using B3LYP functional and 6-31G*(d) basis set. The dispersion correction was em=gd3bj. The solvation model was based on polarizable-continuum model (PCM) and the dielectric constant of G2 was set to be 7.4.

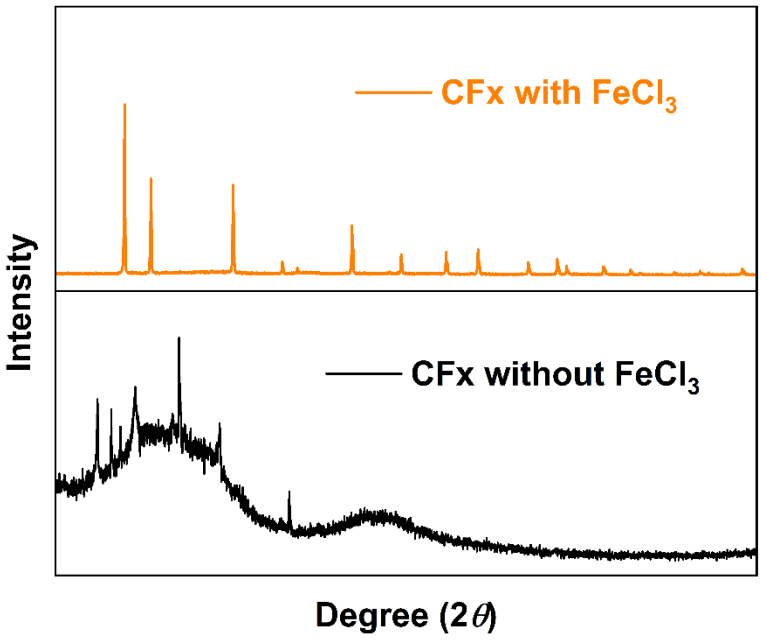

Fig. S1 XRD patterns of synthesis products obtained with and without $FeCl_3$.

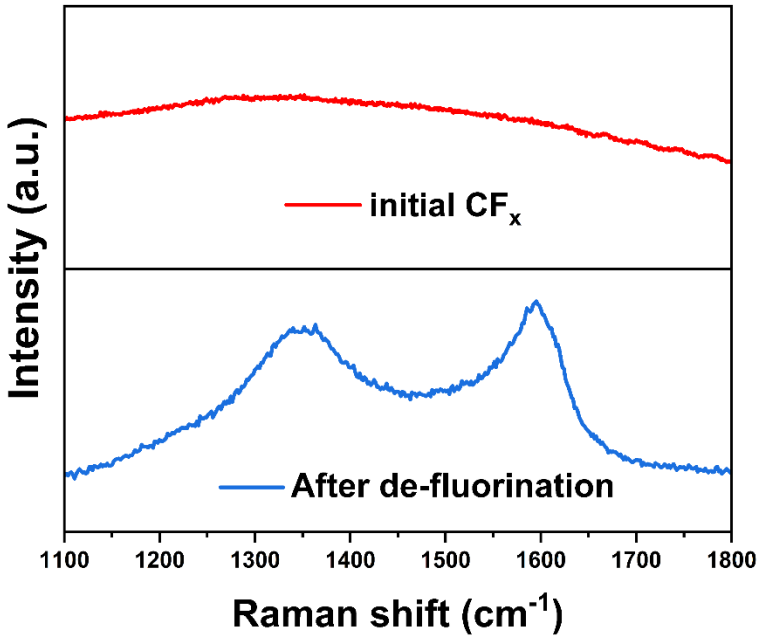

Fig. S2 Raman spectra of CF_x precursor and synthesis product after defluorination.

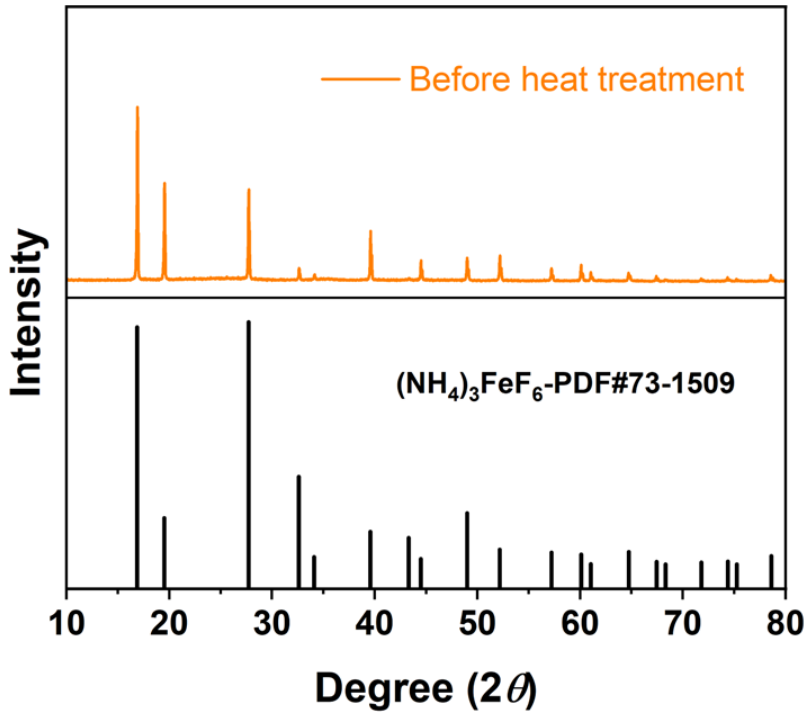

Fig. S3 XRD pattern of synthesis product before heat treatment.

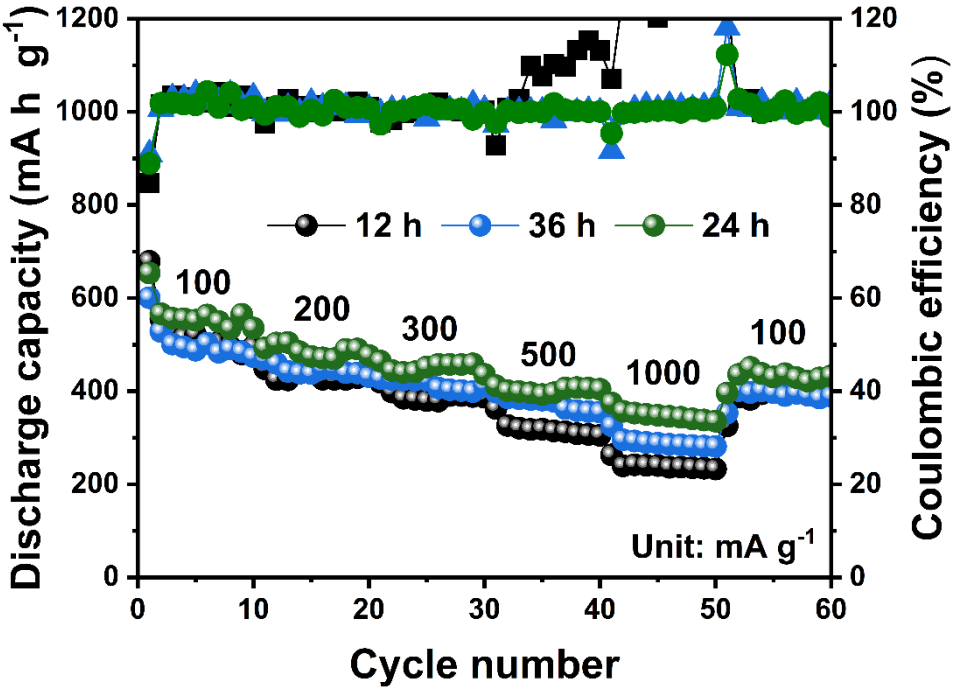

Fig. S4 Rate performance comparison of FF-12, FF-24 and FF-36 cathodes.

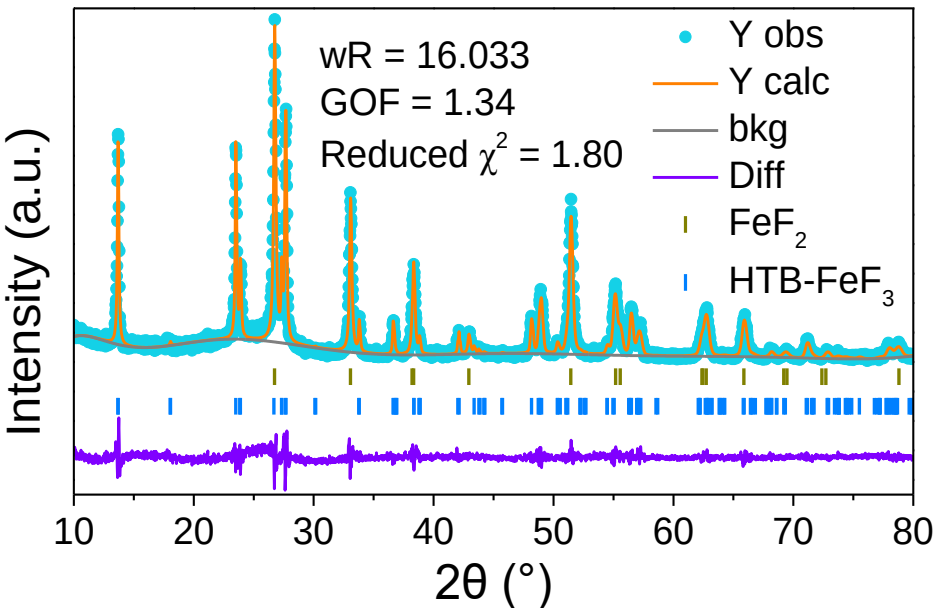

Fig. S5 Rietveld refinement of XRD pattern of FF-24 powder.

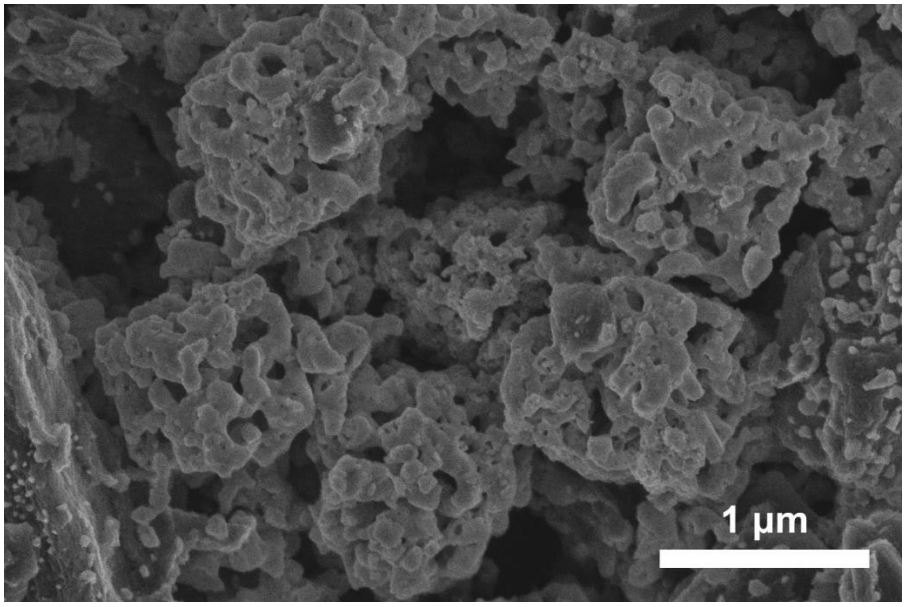

Fig. S6 SEM image of FF-24 powder.

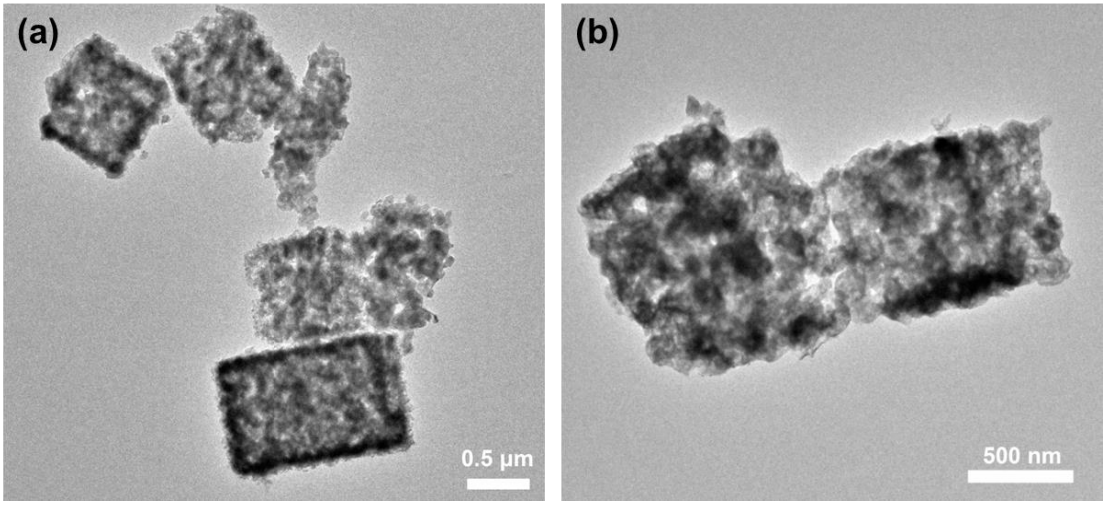

Fig. S7 TEM images of FF-24 in different scales.

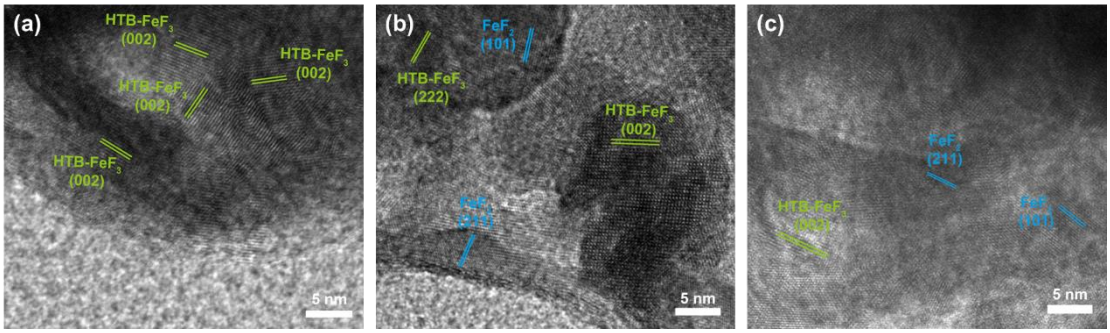

Fig. S8 HRTEM images of FF-24 in different scales.

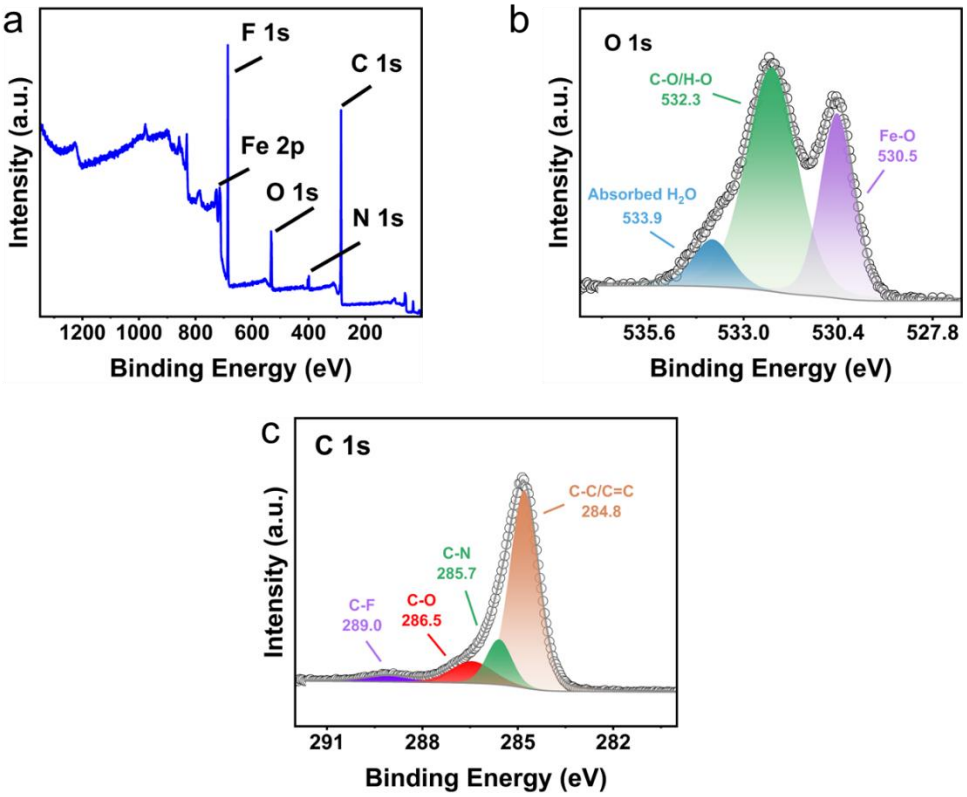

Fig. S9 XPS spectra of FF-24 powder. (a) Overview spectrum. (b) O 1s and (c) C 1s spectra. The C-N peak located at 285.7 eV in C 1s spectrum may stem from the reaction between NH_3 and C, or residual benzylamine.[1] The trace N with lithophilicity on the carbon skeleton benefits to the regulation of Li^+ stripping on the cathode surface during discharging, which is favorable to the uniform distribution of Li^+ in cathode.[2]

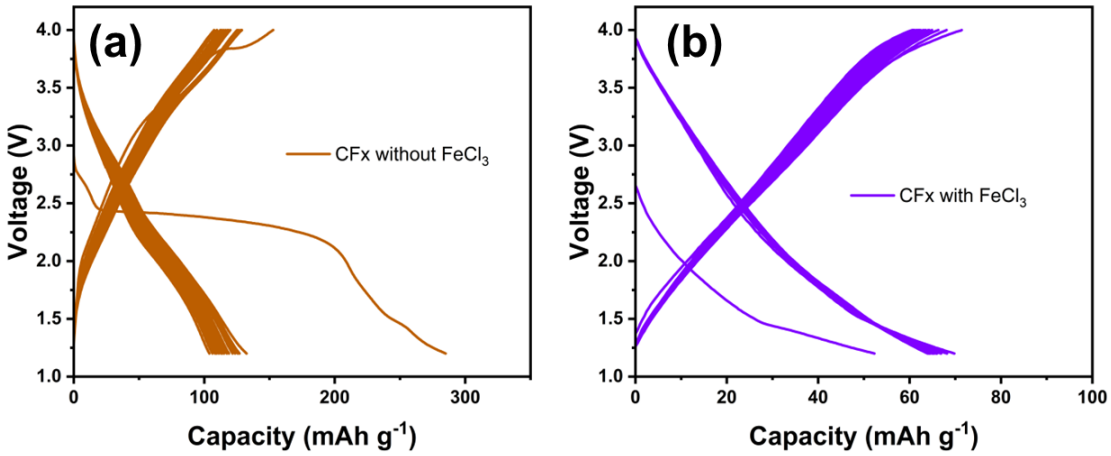

Fig. S10 Galvanostatic charge-discharge curves of defluorinated products of CF_x (a) without $FeCl_3$ and (b) with $FeCl_3$ participation at 100 mA g^{-1}.

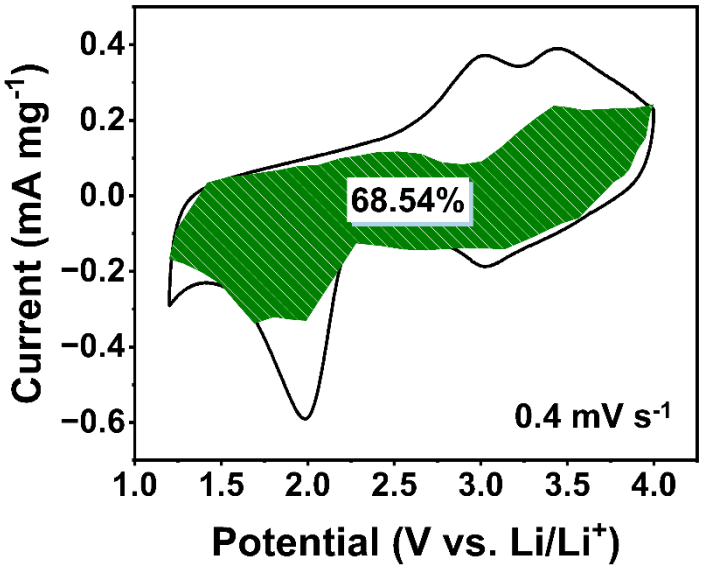

Fig. S11 CV curve of FF-24 cathode at 0.4 mV s^{-1} with capacitive current response (k_1v) outlined in the green area.

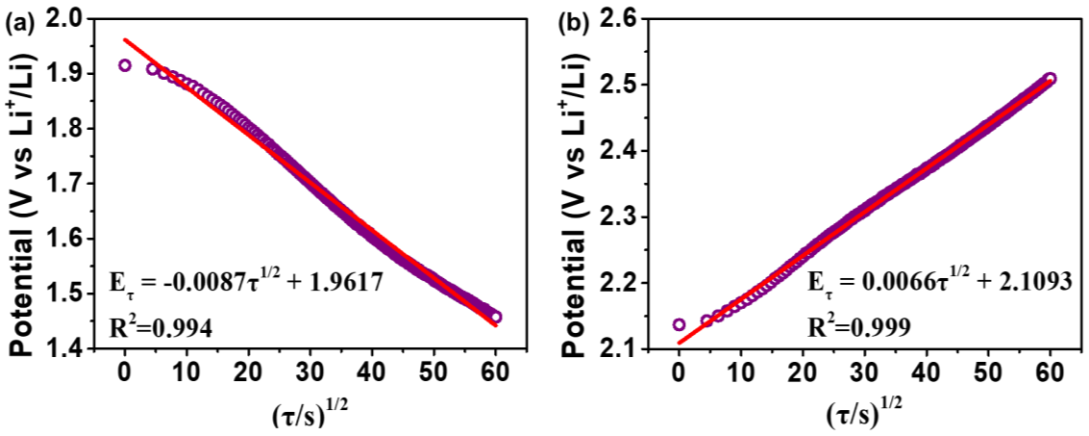

Fig. S12 Linear relationship of transient potential of cell (E_τ) with the square root of titration time (τ) for the single GITT step during (a) discharge and (b) charge processes.

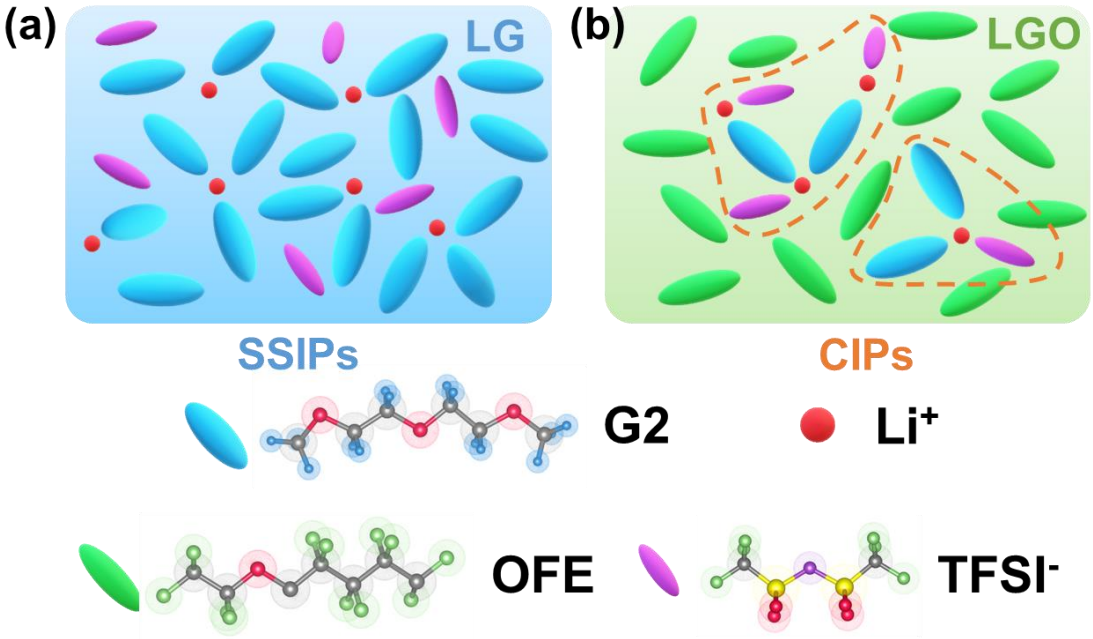

Fig. S13 Schematic illustration of solvation structures of Li^+ ions in (a) LG and (b) LGO electrolytes.

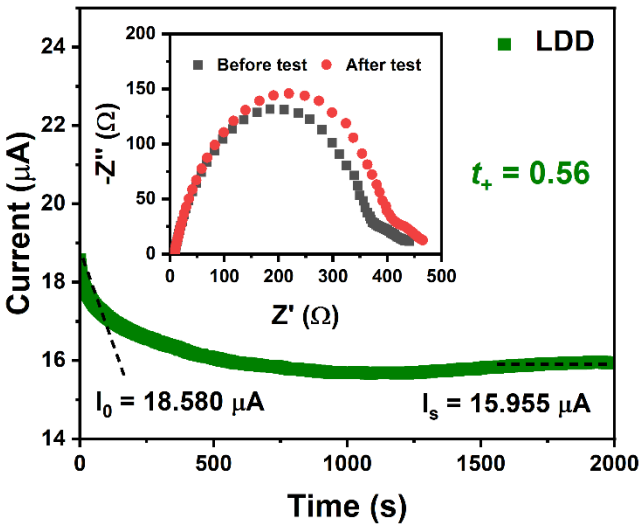

Fig. S14 Constant-voltage (0.01 V) polarization test of Li||LDD||Li cell to estimate the transference number of Li^+. Inset: electrochemical impedance spectra of the cell before and after polarization test.

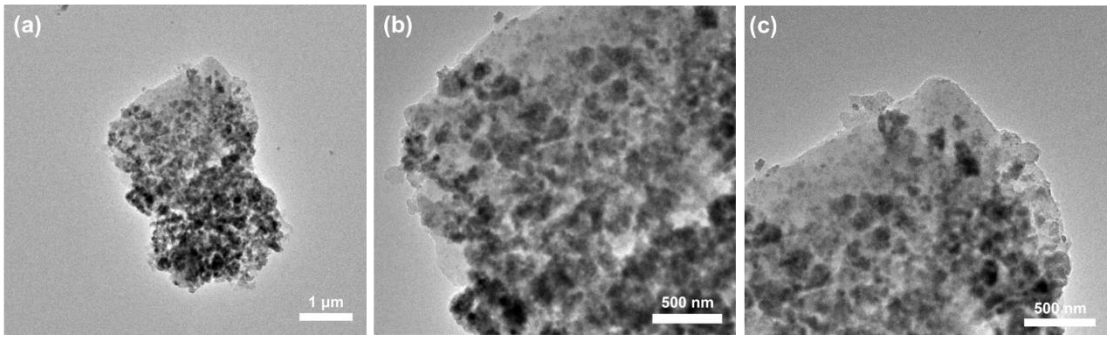

Fig. S15 TEM images of discharged FF-24 cathode in different scales and regions.

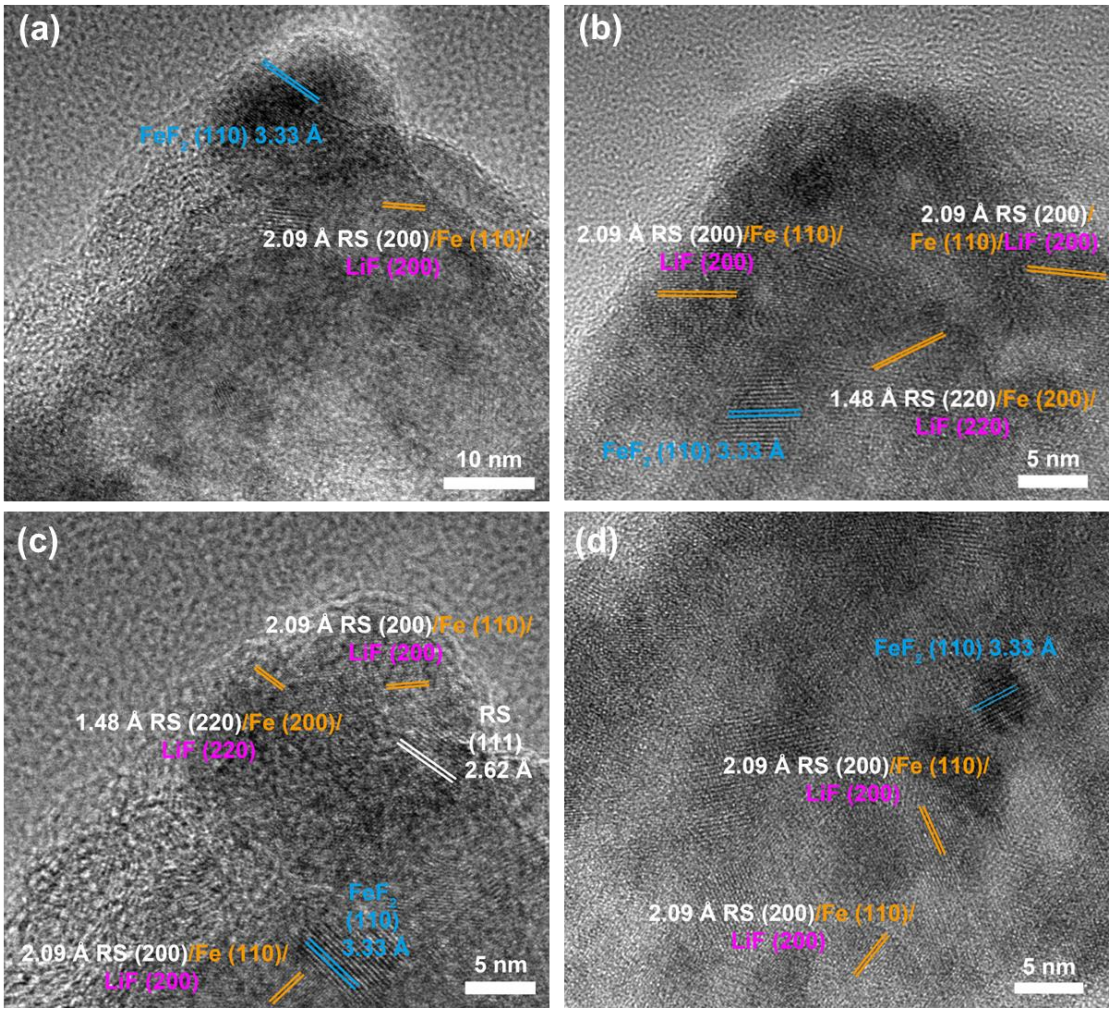

Fig. S16 HRTEM images of discharged FF-24 cathode in different regions. The discharged products of FF-24 contain Fe, LiF, RS phase and FeF_2.

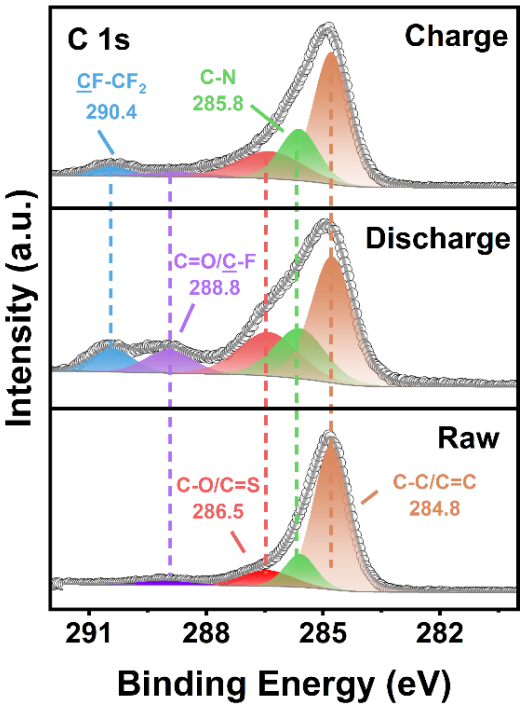

Fig. S17 XPS spectra of C 1s for FF-24 before and after cycling.

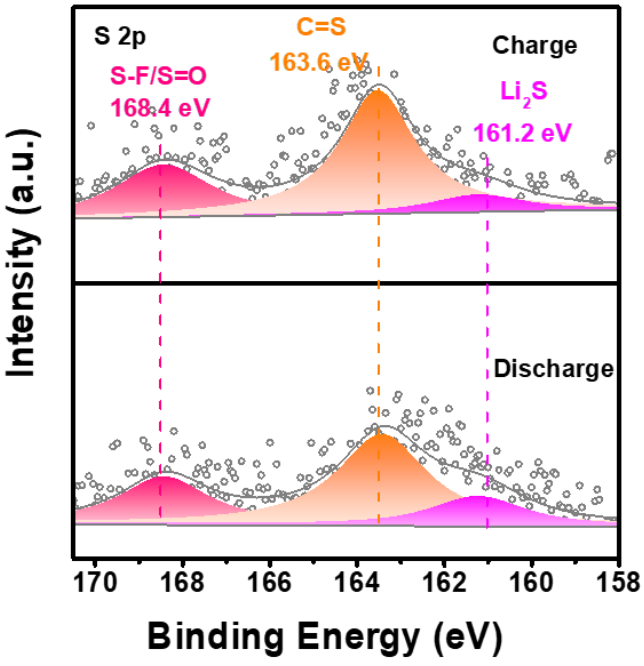

Fig. S18 XPS spectra of S 2p for the cycled FF-24.

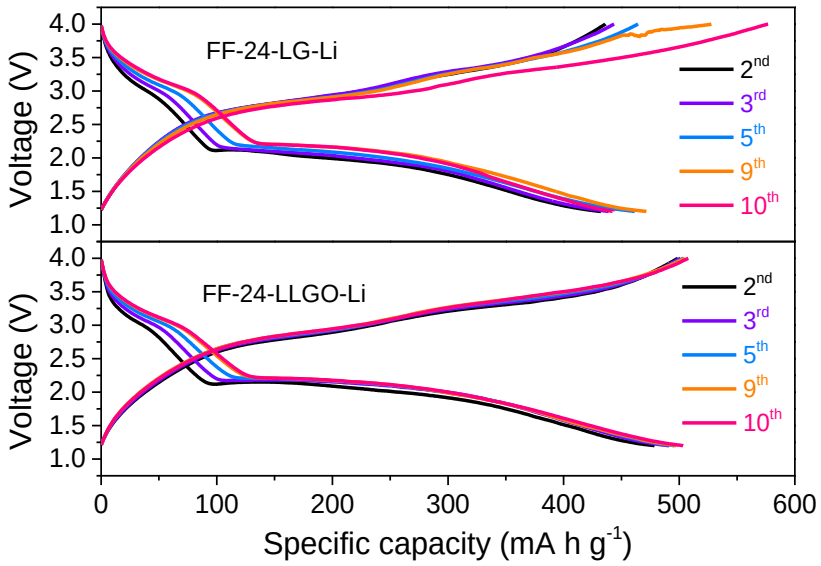

Fig. S19 Electrochemical curves of FF-24|LG|Li and FF-24|LLGO|Li cells at 100 mA g^{-1}.

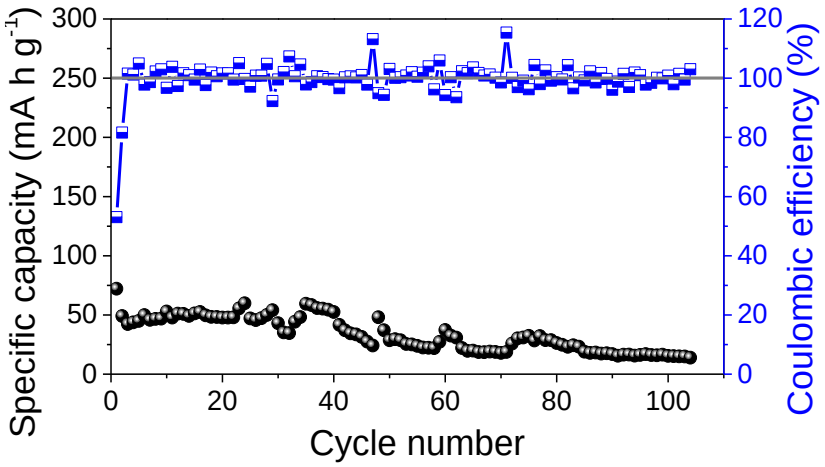

Fig. S20 Cycling performance of FF-24|LLGO|Li cell at 100 mA g^{-1} under harsh conditions (i.e., N/P = 2.8, areal capacity = 2.5 mA h cm^{-2}).

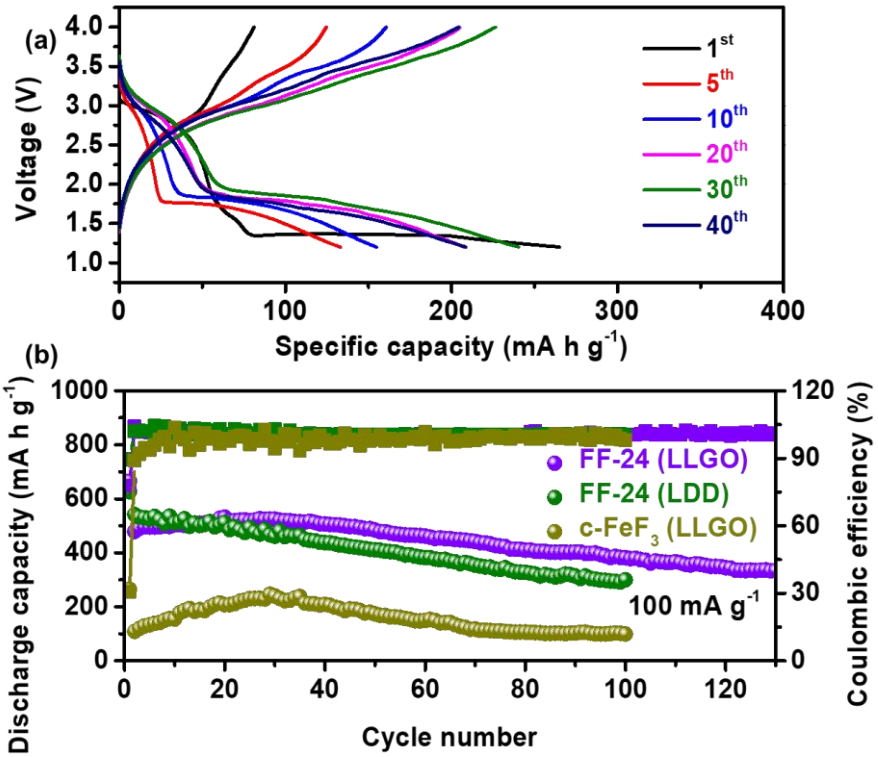

Fig. S21 (a) Electrochemical curves of c-FeF_3|LLGO|Li cell at 100 mA g^{-1} at different cycling stages. (b) Electrochemical cycling performance of c-FeF_3|LLGO|Li, FF-24|LDD|Li and FF-24|LLGO|Li cells at 100 mA g^{-1}.

References

1. Jindal, A.; Basu, S.; P, A. C., Electrospun carbon nitride supported on poly(vinyl) alcohol as an electrocatalyst for oxygen reduction reactions. *RSC Adv.* **2015,** *5*, 69378-69387.

2. Zheng, F.; Yang, Y.; Chen, Q., High lithium anodic performance of highly nitrogen-doped porous carbon prepared from a metal-organic framework. *Nat. Commun.* **2014,** *5*, 5261.